トピックス

What can we learn about dications using threshold photoelectron probes?

P. LABLANQUIE[1], J. H. D. ELAND[2], R. I. HALL[3] and F. PENENT[3]

[1*]*LURE, Centre Universitaire Paris-Sud, 91898 Orsay, FRANCE,*
[2]*Physical and Theoretical Chemistry Laboratory, Oxford OX13QZ, UK,*
[3]*DIAM, Université P. & M. Curie, 4pl. Jussieu 75252 Paris 5, FRANCE*

Molecular dications are exotic species which can have long lifetimes. In order to search for them, to understand the reason for their stability and their decay processes, a number of double photoionisation experiments have recently been developed. We present here a major branch of these experiments with the emphasis on the use of threshold electron spectrometers. We show how they bring insight into the spectroscopy of dications, their dissociation mechanisms and into the double photoionisation process.

1. Introduction

Molecular dications are exotic species that were first observed in mass spectrometers in the twenties. They have attracted great interest because of their presence in the interstellar medium, in the Earth's upper atmosphere and in low temperature plasmas. A strange particularity is that, in spite of the Coulomb repulsion brought by the two positive charges inside the molecular skeleton, they can possess states with long lifetimes; it has been a challenge to characterise experimentally these levels and their structure, to explain how the chemical bond can overcome their propensity to fragment, and to understand their decay mechanisms. However it is only recently, since approximately 10 years ago, that studies of these species have multiplied, with a strong interplay between different theoretical and experimental approaches; a review has been presented by Mathur[1)].

Among the numerous experimental approaches that are being developed to study dications, the most popular one nowadays consists in forming them by double photoionisation from a neutral species; the advantage is that photon transitions impose selection rules that greatly simplify their study. The use of photoionisation also raises fundamental questions on the double photoionisation process; photon absorption being primarily a one electron process, dication production necessarily relies on electron correlations, on which information is sought. As a striking example, the number of experimental and theoretical studies of the most fundamental double photoionisation process, that of He, literally exploded these last few years[2)]. The reason for this recent development is that since double photoionisation is a weak second order process its study necessitates photon sources of high intensity and resolution; the recent development of so-called third generation synchrotrons exactly meets this demand. But the experimental study of dications also relies on coincidence techniques that are essential to characterise double photoionization processes and these coincidence techniques also witnessed an unprecedented progress recently[3)].

In this review, we will present recent development in a special class of these coincidence experiments aimed at the study of dications formed by double photoionisation, experiments in which detection of a《threshold》or low energy electron is involved (typically energy of less than 10 meV). The trick is that such threshold electrons are easily detected with high efficiency and high resolution, making them very efficient probes of ionisation processes. We will present a typical experimental set up that enables coincidence detection of threshold electrons and other particles (electron, ions) formed in the double photoionisation reaction, and show how it can bring information on the spectroscopy, stability, decay process, and formation mechanisms of dications.

2. Experiment

Our experimental set up is presented in **Fig. 1** in its latest configuration. It consists of a photon beam intercepting an effusive gas beam issuing from a 0.4 mm internal diameter capillary tube, and of 3 analysers characterising the particles

* LURE, Centre Universitaire Paris-Sud, Bâtiment 209D, BP 34, 91898 Orsay, France
TEL (+33)1-64 46 80 26 FAX (+33)1-64 46 41 48 e-mail lablanquie@lure.u-psud.fr

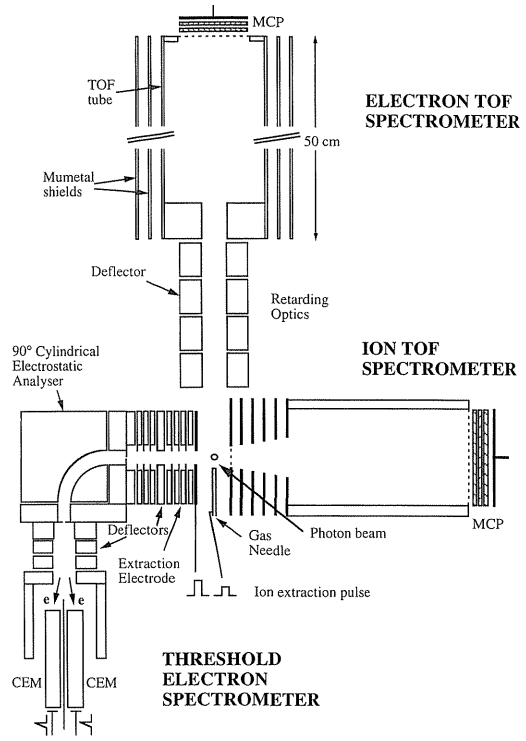

Figure 1. Experimental Set-up.

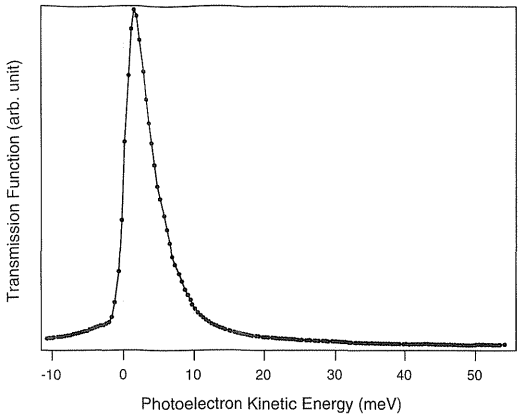

Figure 2. Transmission function of the threshold electron detector. This curve was obtained by measuring the electron signal at Ne 2s ionisation threshold, at the gas phase beam line in Elettra, Italy, photon resolution was around 3 meV. Origin of the energy scale is set at the Ne 2s threshold.

released upon photoionisation. Photons are delivered by the beamlines SA31 or SA72 of the Super ACO synchrotron in Orsay, France or from the Gas Phase beamline of the 3rd generation Elettra synchrotron in Trieste, Italy. The Particle analysers are:

-A threshold electron filter. It has been described in detail in references[4,5] and is based on the penetrating field technique[6]: the field from an extraction electrode in the entrance lens of the analyser penetrates into the scattering centre which is otherwise carefully grounded, the inhomogenuous potential configuration thus created collects very efficiently and guides the low-energy electrons into the lens system; these electrons are then focused at the entrance of a 90° cylindrical electrostatic analyser, where they are filtered from energetic electrons happening to pass through the lens. A second lens system then guides these electrons to the detectors, either 2 channeltrons or a single multi-channel plate assembly; both configurations enable coincidence detection of 2 simultaneously emitted electrons. The performance of this threshold electron analyser is illustrated in **Fig. 2** which shows the transmission of this detector as a function of the kinetic energy of the electron detected. The curve represents in fact the electron yield at the Ne 2s threshold; as we can consider the Ne 2s cross section as constant in this energy range, this curve is, more precisely, the convolution of this transmission function with the photon bandwidth, which was about 3 meV; this causes an apparent maximum for non-zero energy electrons; the shoulder around 5 meV below threshold is attributed to field ionisation of high n Rydberg states; one sees that the effective resolution of this low energy electron filter is around 5 meV. These data were obtained at the Gas Phase beamline of Elettra, Italy. The detection efficiency for 0 eV electrons was measured to be around 45%.

-An ion time-of-flight spectrometer; it is described in reference[7] and has been designed with 2nd order focusing properties, as presented by Eland[8]. It is operated in coincidence mode: upon detection of an electron (or a pair of electrons) by the threshold electron analyser, a positive extraction pulse is applied on both the gas needle and the electrode limiting the source region on the threshold electron analyser side, thus pushing the ions created towards a 40 mm diameter micro-channel plate assembly. The detection efficiency for ions was measured to be around 25%.

-An electron time-of-flight spectrometer; it is described in reference[9] and is based on the retarding field principle[10]: a four-elements entrance lens allows focussing of electron trajectories to optimize collection efficiency, the electrons are slowed down into the time-of-flight zone in which they develop a longer time of flight, suitable for better energy resolution. Time of flight of the electrons is measured with respect to the photon pulse, in the 2 bunch operation mode of the Super ACO ring (inter light pulse duration is then 120 ns).

An essential characteristics of the experimental set up is its capability of detecting in coincidence several particles emitted from the same ionisation event of a single molecule: 2 threshold electrons, or 1 threshold electron plus an energetic electron, or 1 (or 2) threshold electron(s) plus the associated 1 (or 2) ions.

3. Spectroscopy of Dications investigated with Threshold Photoelectrons Coincidences (TPEsCO)

Release of 2 threshold photoelectrons upon photoionisation implies that the photon energy coincides with a double ionisation threshold; hence the spectrum of doubly charged

levels can simply be obtained by detecting the yield of such coincidences between 2 threshold photoelectrons as a function of the photon energy (TPEsCO spectrum). The great advantage of this method is the high resolution of the threshold electron detector (around 5 meV here, see **2**) so that the final resolution is determined by the photons only, which is generally of the order of a few tens of meV in our experiment in Super ACO, but the emergence of beamlines of higher brilliance on 3rd generation synchrotrons open up the possibility to push down this limit. This method was discovered in 1992, independently by Hall et al[11] and Krässig and Schmidt[12], it has enabled exploration of the spectroscopy of a range of dications with unprecedented resolution[13]. We will illustrate this with 2 examples.

3.1 Proof of principle: TPEsCO spectra of Ar Atoms

Figure 3b) shows a TPEsCO spectrum of Argon. It was obtained at Beamline SA31 in Super ACO with a 30 meV photon resolution. The first 2 electronic states of Ar^{++} as well as the spin orbit components of the Ar^{++} ^3P state are clearly resolved. But the striking point is that the intensities of the lines are far from statistical. The explanation was first given by Krässig and Schmidt[12], and is illustrated by **Fig. 3**a); it gives the yield of threshold photoelectrons, or TPE spectrum of Ar in the same energy region, and reveals the highly excited singly charged Ar^+ states present in this region. They are mainly high Rydberg states converging onto higher Ar^{++} thresholds. The accidental coincidence of one such Rydberg state with an Ar^{++} state considerably enhances the TPEsCO signal for that particular Ar^{++} state; the process is an indirect double ionisation route passing through that Rydberg state that subsequently autoionizes:

$$h\nu + Ar \rightarrow A^{+*}(\text{Rydberg}) + e^-_{\text{photoel.}}\ (Ec=0)$$
$$\rightarrow Ar^{++} + e^-_{\text{Auger}}\ (Ec=0) + e^-_{\text{photoel.}}\ (Ec=0) \qquad (1)$$

It is seen that such an accidental coincidence occurs for Ar^{++} $^3P_2$ and $^3P_0$ states, which are respectively degenerate in energy with $3p^{-2}(^1D)7p$ and $3p^{-2}(^1D)6f$ Rydberg states, but not for Ar^{++} $^3P_1$ and ^1D states.

This process incidentally explains why the TPEsCO technique can work at all: the direct double ionisation cross section is expected to be exactly zero at threshold, and only indirect processes can explain the appreciable signals.

Finally, note that the TPE spectrum in **Fig. 3**b) is dominated by Rydberg states of high angular momenta; all are $3p^{-2}$ (^1D) nl configurations with l=f or g. Krässig et al[14] explained this in the frame work of the Wannier picture, as first predicted by Fano in 1974[15].

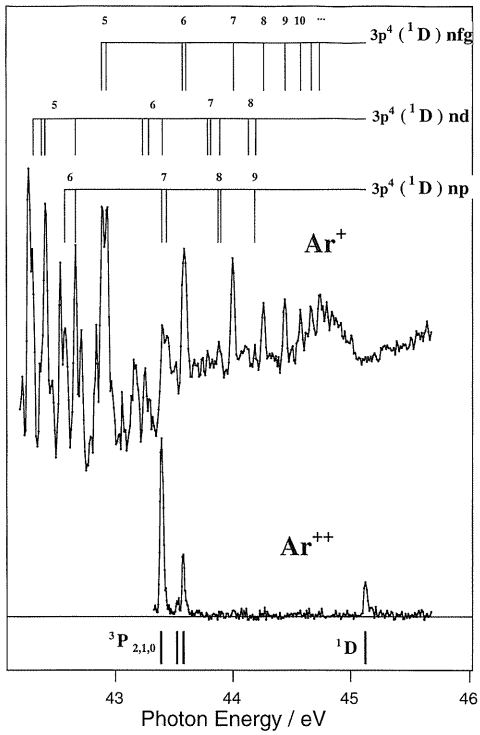

Figure 3. (a) Yield of threshold photoelectrons (TPE spectrum) and (b) yield of coincidences between 2 threshold photoelectrons (TPEsCO spectrum) for Argon.

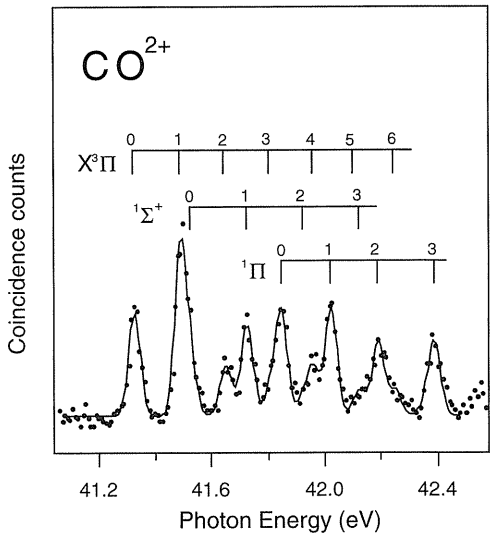

Figure 4. TPEsCO spectrum for CO (Ref. 7).

3.2 Vibrational levels of molecular dications revealed by TPEsCO spectra

The spectroscopy of atomic dications is well established, but vibrational levels of molecular dications were unknown, except for a few cases, until TPEsCO technique revealed them. **Figure 4** shows a TPEsCO spectrum for CO[7], it is remarkable that the 3 vibrational progressions coeeesponding to the 3 CO^{++} electronic states present in this energy region can be observed, even if they lie outside the Franck-Condon region. This has to be attributed to an indirect process of the same kind as observed for Ar; highly excited CO^{+*} Rydberg states are formed at threshold and further autoionise, releasing a threshold Auger electron. These excited CO^{+*} Rydberg sates can have a lifetime sufficient to let them vibrate before they autoionise; in this way CO^{++} vibrational

levels outside the Franck-Condon region can be efficiently populated. Note that this indirect double ionisation mechanism at threshold is general, and was also observed in triatomic molecules such as CS_2[16].

The above consideration also implies that, contrary to the Born-Oppenheimer approximation, nuclear motion can precede electron emission. Vibrational motion prior to autoionisation has been invoked to explain the intensities of unexpected M^{++} vibrational levels in TPEsCO spectra, but molecular dissociation prior to autoionisation is a well established process. In double photoionisation at threshold it was first observed to occur in H_2O[17]: in this way dissociative double ionisation can take place well below the threshold one would expect, considering the position of doubly charged states in the Franck-Condon region. The molecule in which this process has been the subject of the most experimental investigations is CO, see **5.1**, but such a process does not show up in the CO TPEsCO spectrum, as the second Auger electron is not a low energy one[18]; the situation is different in H_2S, where the TPEsCO spectrum presents a continuum below the peaks associated to the first H_2S^{++} vibrational states; this continuum was attributed to the formation at threshold of H_2S^{+*} Rydberg states which dissociate prior to releasing a low energy electron[19].

4. Stability and Dissociation Mechanisms of Dications investigated with Threshold Electron Pair Ion Coincidences (TEPIC)

Observation of vibrational peaks in a TPEsCO spectrum proves that the considered level of the doubly charged ion has a lifetime τ in excess of the vibration time, typically $\tau > 10$ fs. However dications can have states with lifetimes in excess of several seconds[20]; the question is then raised how to estimate the lifetime of the vibrational levels revealed in TPEsCO spectra, in this huge time range that can extend from 10 fs up to seconds or even days, and to understand the mechanisms for their stability and eventual decay. An experimental technique was proposed recently to answer these points, it combines the TPEsCO spectroscopy with ion time-of-flight spectroscopy[7]: well-defined dication vibrational states are prepared at threshold and selected by detection of their 2 associated threshold electrons; their stability or dissociation dynamics is then observed by coincidence detection of the parent or fragment ions. Note that this experiment involves, for a diatomic molecule, the coincident detection of 3 to 4 particles depending on whether the dication fragments or not.

Figures 5 and **6** illustrate this Threshold Electron Pair Ion Coincidence (TEPIC) technique in the CO case. 3 particle (2 electrons +1 ion) coincidences are presented in **Fig. 5**; comparison with simulated spectra enables one to extract the kinetic energy released upon dissociation and the lifetime τ of the levels. The lifetime τ is respectively > 10 ps, 200 ± 100 ns, 700 ± 200 ns and < 100 ns for the levels $X^3\Pi$ v=1 or $^1\Sigma^+$ v=0, $X^3\Pi$ v=2, $^1\Sigma^+$ v=1 and $^1\Pi$ v=1 considered in **Fig. 5**. It is seen that this TEPIC technique is especially sensitive for lifetimes τ in the time window [100 ns–10 μs]; other techniques explore other time windows: for instance, the Doppler free kinetic energy release spectroscopy introduced by Lundqvist et al[21] is sensitive for $\tau < 100$ ns. Ion storage rings[20] at the other extreme measure lifetimes in the range of seconds.

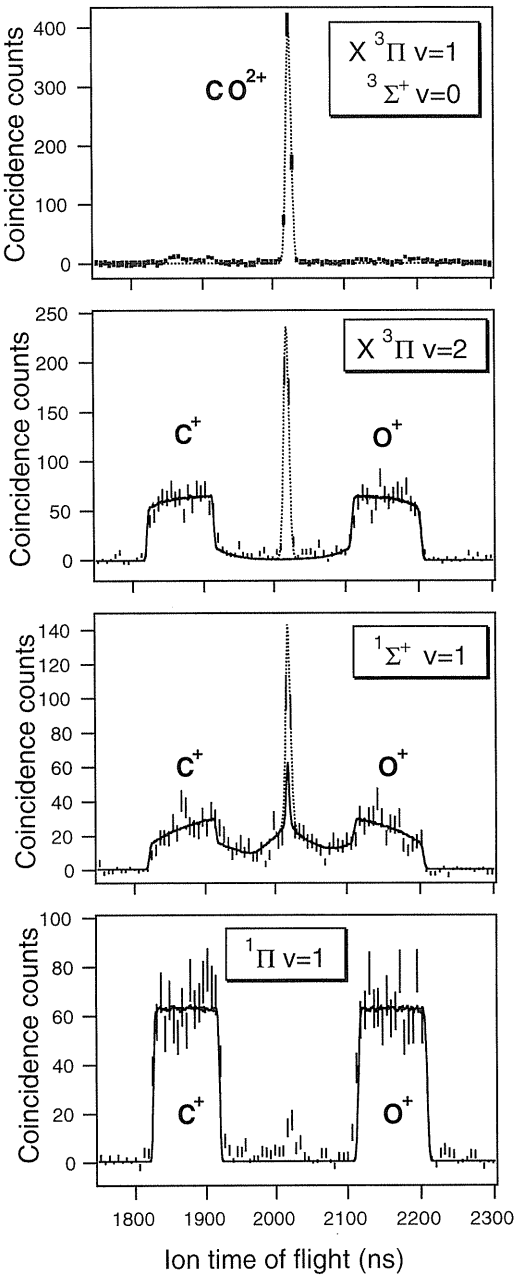

Figure 5. TOF spectra of the ions resulting from formation of the indicated levels of CO^{2+} and corresponding to coincidences between 3 particles, 2 electrons and 1 ion. The full lines are simulated spectra with which the lifetime of the levels can be obtained. (Ref. 7).

Kinetic energy release Er can be deduced from the spread in time-of-flight of the C^+ or O^+ peaks in **Fig. 5**; note that the information is the same in both as they are correlated as issuing from dissociation of the same dication parent: $CO^{++} \rightarrow C^+ + O^+$. This is demonstrated in **Fig. 6** that represents the 4 particle (2 electrons+2 ions) coincidences.

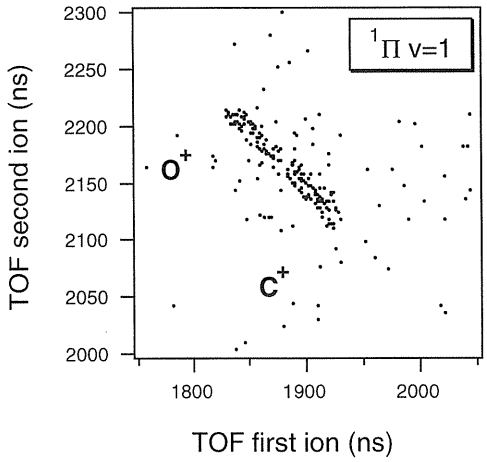

Figure 6. TOF spectrum of C^+ and O^+ ions resulting from dissociation of the $^1\Pi$ v=1 state, and corresponding to coincidences between 4 particles, 2 electrons and 2 ions. (Ref. 7).

The Er value gives the dissociation limit which is reached, we find that the ground state $C^+(^2P)$ and $O^+(^4S)$ fragments are formed in each case, this is consistent with the theory predicting that the lifetime of all the discrete vibrational levels known for CO^{2+} is determined by the coupling to a single dissociative state, the $^3\Sigma^-$ state correlated to ground state $C^+(^2P)$ and $O^+(^4S)$ fragments.

5. Indirect double photoionisation processes investigated with coincidences involving one threshold photoelectron

5.1 Threshold electron/ion coincidence experiments

The threshold photoelectron/ion coincidence (TPEPICO) technique is widely used for the investigation of singly charged ions (see Ref. 22 for a review); it consists in preparing a well defined vibronic level of a singly charged molecular cation at its ionisation threshold; this is assured by detecting the associated threshold photoelectron. The stability or dissociation of this level is then observed by detecting in coincidence the parent or fragment ions. In a sense the TEPIC technique presented in **4** is the extension of TPEPICO from the monocations to the dications. Yet the use of TPEPICO in the energy range corresponding to the double ionisation thresholds can offer a wealth of information on the singly charged highly excited states whose binding energies lie in this energy range; note that it is such excited monocations that are responsible for the indirect double ionisation paths revealed in TPEsCO spectra (see **3**).

We will illustrate this point with CO as an example. **Figures 7** and **8** show TPEPICO spectra obtained at $h\nu=42$ and 40 eV respectively. They show the fate of the highly excited CO^{+*} states of 42 and 40 eV binding energy; 3 possibilities arise:

-1) the CO^{+*} state dissociates to $C^+ + O$ or $C + O^+$. No evidence for formation of stable (lifetime > 100 ns) CO^+ species was found.

-2) the CO^{+*} state autoionises to stable CO^{++} vibrational levels; we saw in **4** that it could only be $X^3\Pi$ v=0, $X^3\Pi$ v=1 or $^1\Sigma^+$ v=0. It gives rise to the detection of a CO^{++} ion. Note that, as expected, no CO^{++} ion is formed at $h\nu=40$ eV, (**Fig. 8**), because the excitation energy is not enough to reach these CO^{++} levels.

-3) the CO^{+*} state autoionises to predissociating or dissociative CO^{++} states giving the reaction $CO^{+*} \rightarrow C^+ + O^+ + e$. In this case a pair of C^+ and O^+ correlated ions are formed, and they will appear in 3 particles coincidences (1 threshold electron, C^+ and O^+); this is demonstrated in **Figs. 9** and **10**. Note the weak tail in **Fig. 9** at $h\nu=42$ eV, connecting the C^+/O^+ TPEPIPICO bar to their CO^{++} parent, it is a well known "metastable tail"[23]; it corresponds to autoionisation processes to the metastable $^1\Sigma^+$ v=1 level, as demonstrated in **4**, and is found to disappear at $h\nu=40$ eV, (**Fig. 10**), because once more the excitation energy is not enough to reach this CO^{++} level.

The contribution of the dissociative autoionisation processes to the raw TPEPICO spectra in **Figs. 7**a) and **8**a) can

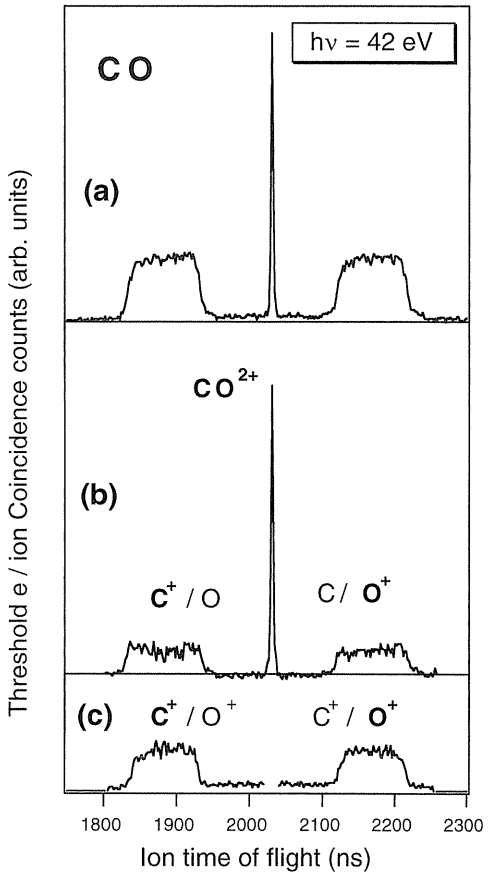

Figure 7. TOF spectrum of the ions resulting from time evolution of highly excited CO^+ states of binding energy 42 eV; they have been obtained by coincidences between 1 threshold electron and 1 ion in CO at $h\nu=42$ eV. a) is the raw spectrum. c) displays the contribution in Fig. 7a) of dissociative autoionisation processes, it was deduced from Fig. 9 taking into account ion detection efficiencies. b) is the difference spectrum, and displays processes where one ion only (CO^{++}, C^+ or O^+) results from the time evolution of the initially formed CO^+ state; it represents contribution in Fig. 7a) of dissociation and autoionisation processes to CO^{++} levels that are stable on the experimental time window ($>10\,\mu s$).

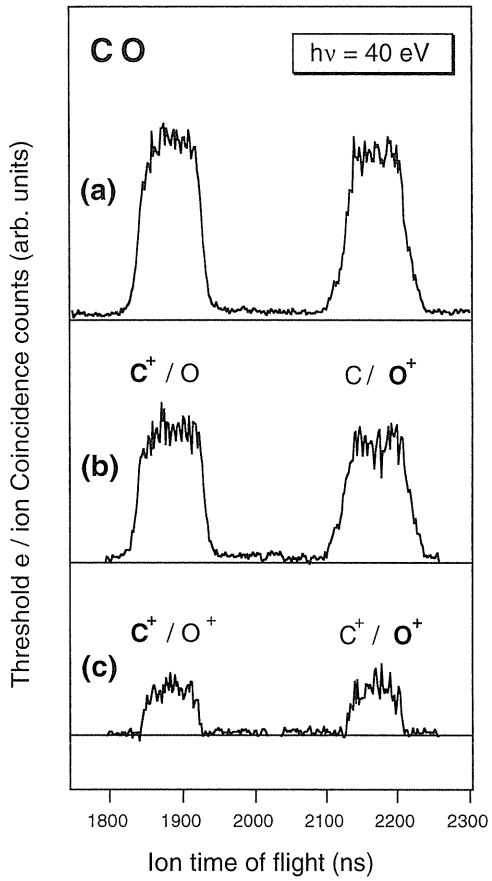

Figure 8. CO. Same as Figure 7, but at hν=40 eV.

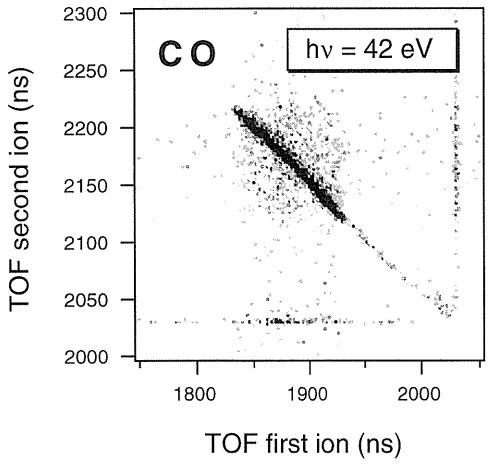

Figure 9. TOF spectrum of C^+ and O^+ ions resulting from dissociative autoionisation of highly excited CO^+ states of binding energy 42 eV; they have been obtained by coincidences between 1 threshold electrons and 2 ions for CO at hν=42 eV.

easily be deduced from the simultaneously measured **Figs. 9** and **10**, by taking into account the ion detection efficiency of 25% (see **Figs. 7**c) and **8**c)). **Figures 7**b) and **8**b) show the subtracted TPEPICO speetra obtained by the subtraction of the curves in **Figs. 7**a) and **8**a) by those in **Figs. 7**c) and **8**c), which reveal the contribution of processes 1) and 2).

Comparison of the widths of C^+ and O^+ peaks in **Figs.**

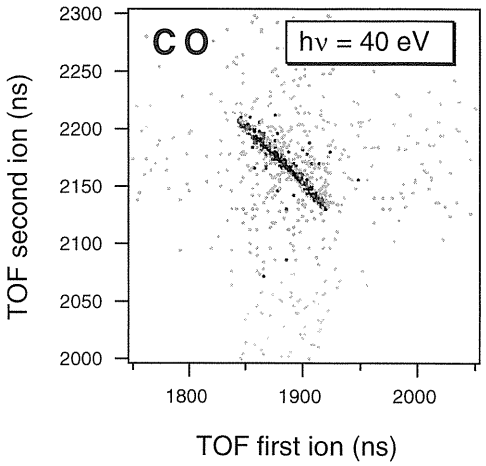

Figure 10. TOF spectrum for CO. (same as Fig. 9) at hν=40 eV.

8b) and **8**c) shows that the kinetic energy release is less upon dissociative autoionisation than upon simple dissociation, in other words, kinetic energy release is less for dissociation of a doubly charged CO^{++} ion than for dissociation of a singly charged CO^{+*} ion, in this particular condition. This can be surprising if we think of the strength of Coulomb repulsion, but it is naturally explained by considering the low excess energy with respect to the lower $C^+(^2P)+O^+(^4S)$ dissociation limit at around 36 eV; furthermore the process here necessarily implies nuclear motion prior to electron ejection, and the distance between the C^+ and O^+ partners at the moment of the "localisation" of the 2 positive charges is large enough to decrease the coulomb repulsion. Note that precise measurement of the widths of the peaks gives the kinetic energy released upon dissociation, it is then possible to deduce the kinetic energy of the Auger electrons by energy conservation considerations. Such a measurement was not attempted here, because of the low resolution, but an alternative method consists in directly measuring the kinetic energy of the Auger electron, in a threshold electron/Auger electron coincidence experiment. This was done by Thompson et al[18] who found in fact that the Auger electron mainly corresponded to an O^+ Auger electron, that is, dissociation is completed before ejection of the Auger electron:

$$CO^{+*} \rightarrow C^+ + O^* \text{ and then } O^* \rightarrow O^+ + e^- \qquad (2)$$

Branching ratios between the different possible decay paths of excited CO^{+*} states are represented in **Fig. 11** as a function of the internal energy of the CO^{+*} state. They have been deduced from 2 and 3 particle TPEPICO coincidence spectra such as the ones in **Figs. 8** and **10**, with the procedure presented above. The experiment was performed on beamline SA31 at Super ACO, with a photon resolution of around 50 meV. One can notice the decreasing importance of the $C^+ + O$ and $C + O^+$ dissociation channels, when the intensity of doubly charged ions increases, thus facilitating autoionisation; a change of slope is observed around 41.6 eV in the $C^+ + O^+$ channel, when predissociated CO^{++} levels can be reached, similarly the CO^{++} channel presents a step-

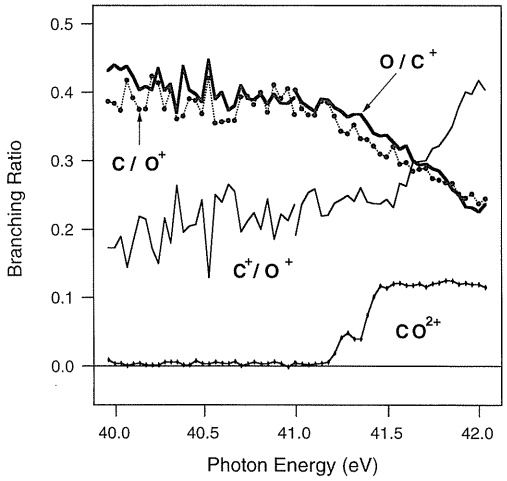

Figure 11. Branching ratios showing the evolution of decay paths of highly excited CO^+ states, as a function of their internal energy; they have been deduced from threshold electron/ion(s) coincidences such as shown in Figs. 7 to 10.

wise behaviour at the opening of the stable CO^{++} vibrational levels; the existence of the second step at the opening of the unresolved $X^3\Pi$ v=1 and $^1\Sigma^+$ v=0 states also demonstrates that CO^{+*} Rydberg states converging to them escape vibrational autoionisation to the CO^{++} $X^3\Pi$ v=0 level.

Similar investigations of the fate of highly excited cations in the vicinity of double ionisation thresholds have been done in CS_2, SO_2 and CO by Field and al[24] with a different technique, that uses fixed energy HeII photons, and coincidence detection of an energetic electron and the associated ions; the principle of the experiment is the same, except that the excited cations are no longer formed at their threshold.

5.2 Threshold electron/electron coincidence experiments

The first electron/electron coincidence experiment applied to double photoionisation[25] involved detection of a threshold electron: in this way high detection efficiency could be reached, that was necessary in view of the low cross section of the process. Since then, progress in coincidence techniques and synchrotron sources has made possible much more sophisticated experiments where not only energies but also emission angles of both electrons are measured; even very tenuous phenomena, such as the direct double ionisation of He near its threshold are investigated in great detail [see 2 and 26 for a review]. However, these experiments have been mainly devoted, up to now, to the study of double photoionisation of atoms. No doubt that extension to molecules will very soon bring detailed information on the dynamics of molecular dication formation by photon impact, which the first pioneer experiments on O_2[27] and H_2[28] have begun to reveal.

In molecules, the threshold electron/electron coincidence technique is still at its beginning; as described in **3.1**, it brought insights into the dynamics of double photoionisation at threshold in CO[18]; such experiments have recently been extended to the case of O_2, and also demonstrated that emission of the second electron can await the complete dissociation of the initially formed cation[29].

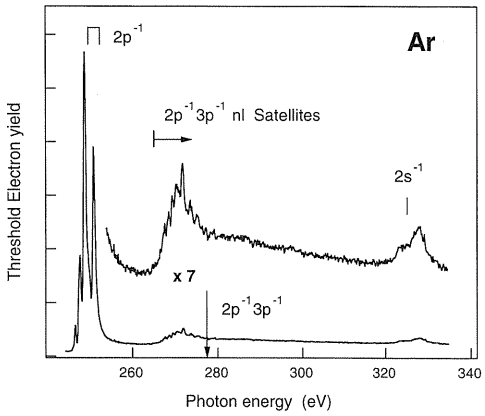

Figure 12. Yield of Threshold Electrons in the vicinity of Ar 2p and 2s thresholds (Ref. 9).

6. A new spectroscopic technique for dications: Auger/Threshold Photoelectron Coincidence Spectroscopy

Threshold electron/electron coincidence techniques can be applied to study not only valence double ionisation but also innershell photoionisation. In this case the energetic electron is an Auger electron, and the signal is greatly enhanced with respect to the《direct》valence regime. Interest is twofold:

-1) choice of a threshold photoelectron issuing from a well-defined innershell level enables filtering of the Auger spectrum, and the lines corresponding to that innershell level to be specifically displayed.

-2) Coincidence detection of the 2 emitted electrons exactly defines the state of the dication formed; from energy conservation considerations, it can be shown that the resolution achieved is not limited by the innershell hole lifetime: it is thus possible to achieve high resolution spectroscopy of the dication formed by Auger decay.

We will now illustrate these 2 points with the example of Ar L shell photoionisation[9]. **Figure 12** shows the yield of threshold electrons as a function of photon energy in the vicinity of the Ar L shell edges. This spectrum reveals structure due to excitation and ionisation, associated with 2p, 2p satellites and 2s holes. Note that in a threshold spectrum, the ionisation peaks are shifted from their nominal binding energy by post-collision interaction (PCI)[26]. Upon 2p or 2s ionisation, Auger decay takes place and leads to Ar^{++} levels as illustrated in **Fig. 13**: 2p holes give the Ar $L_{2,3}MM$ Auger lines, while 2s holes produce dominantly the Ar $L_1L_{2,3}M$ Coster-Kronig lines; in this case the Ar^{++} states formed by the Coster-Kronig decay still contain an innershell 2p hole and further emits a cascade Auger electron to Ar^{3+} final states. As a result, **Fig. 13** shows that different Auger lines, corresponding to the different deexcitation branches, are expected around 200 eV; it is not easy to disentangle them in a simple, non-coincident Auger spectrum, and a careful choice of the excitation conditions is necessary to visualise the weak cascade Auger lines associated with the 2s hole[30].

By contrast, measurement of the Auger spectrum in coincidence with the photoelectron immediately filters the lines according to the hole they are associated with, as is demonstrated in **Fig. 14**. Note the sensitivity of the technique, that reveals the ArL_1MM Auger lines around 280 eV.

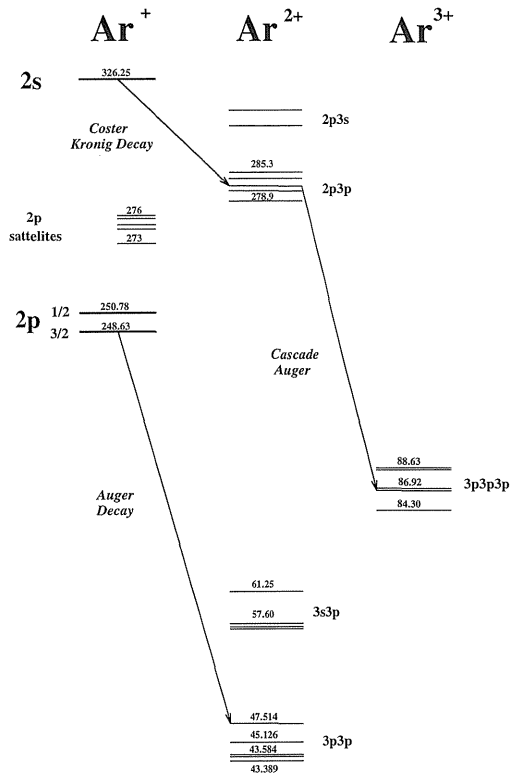

Figure 13. Energy Levels of Ar^+, Ar^{2+} and Ar^{3+} ions involved in the experiment.

Figure 15a) shows the Ar^{++} $2p^{-1}3p^{-1}$ states formed by the $L_1L_{2,3}M_{2,3}$ Coster-Kronig transitions. Comparison with the 'non-coincident' Auger spectrum of Mehlhorn[31] demonstrates, as expected, the absence of broadening due to the 2s hole lifetime (2.25 eV). The total experimental resolution amounts to 650 meV and is exclusively determined by the photons. Comparison with calculations in **Fig. 15**b) enables the peaks to be attributed to well defined $Ar^{++}2p^{-1}3p^{-1}$ states: their spectroscopy, hidden in the non-coincident Auger spectrum is now clearly revealed.

A closer inspection of **Fig. 15**a) reveals intensity for energies greater than 48 eV, where no Ar 2s decay lines are expected. In order to understand their origin, a complete coincident spectrum is presented in **Fig. 16**a); one recognises the Ar $L_1L_{2,3}M$ Coster-Kronig lines around 45 eV, the Ar $L_{2,3}$ MM cascade Auger lines around 200 eV and the Ar L_1MM Auger lines around 280 eV, as seen in **Fig. 14**. There is also an extra doublet peak corresponding to 2p photoelectrons, as is evident by comparison with the non-coincident electron spectrum of **Fig. 16**b). This threshold electron/energetic 2p photoelectron coincidence suggests that the threshold electron is in this case an Auger line; in fact it was observed in coincident spectra measured in the case of Xe 4d ionisation[32], that double Auger, i.e. simultaneous emission of two electrons which randomly share the available energy, and/or cascade Auger transitions can result in the emission of threshold Auger electrons. Similarly, one also expects coincidences between threshold Auger electrons and 2p satellite photoelectrons, and they appear around 50 eV kinetic energy, as revealed by the comparison of **Figs. 16**a) and **16**b); the contribution of this process has been estimated from the non-coincident spectrum **Fig. 16**b) and is presented in **Fig. 15**a) and **16**b) (full lines).

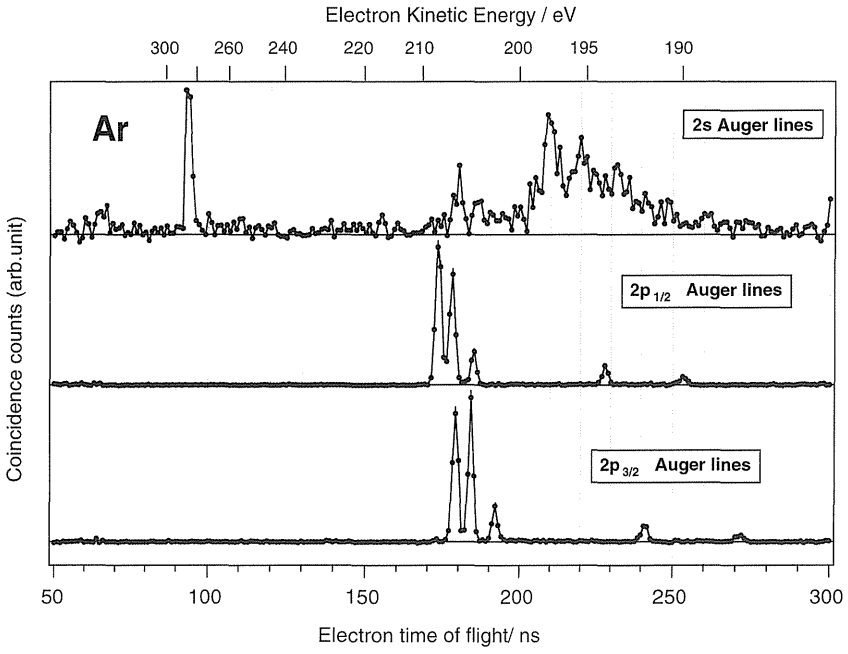

Figure 14. Pure Auger spectra associated to Ar 2p and 2s holes. They have been obtained by Auger-Threshold Photoelectron coincidences with the photon energy set at the maximum of the corresponding threshold photoelectron peaks.

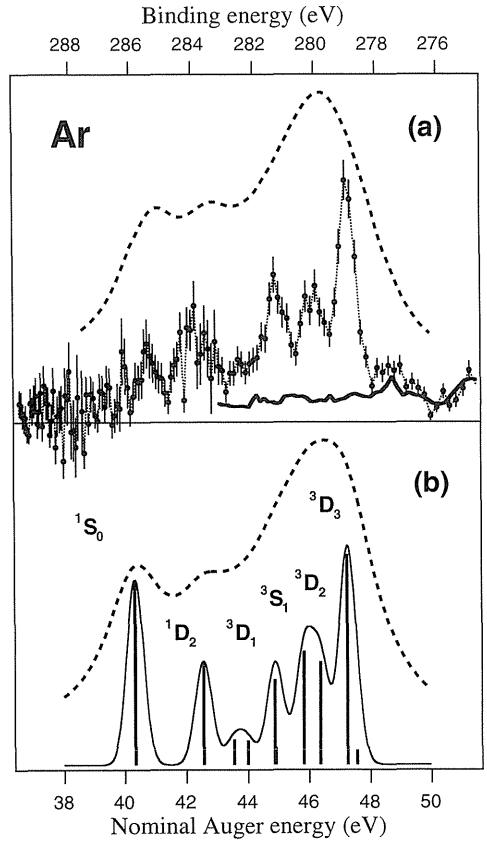

Figure 15. (a) $L_1L_{2,3}M_{2,3}$ Coster-Kronig lines measured in coincidences with Ar 2s photoelectrons at $h\nu=327.5$ eV, compared with the non-coincident Auger spectrum from Ref. 31. (dotted line). The "nominal" Auger electron energy corresponds to the measured coincident Auger electron energy corrected for the PCI shift, Δ(PCI), where Δ(PCI)=$h\nu$-Binding Energy (Ar^+ 2s). (b) The theoretical calculations (sticks) convoluted with a 650 meV Gaussian function corresponding to the experimental resolution (full line), and convoluted with a 2.25 eV Lorentzian function corresponding to the non-coincident Auger spectrum (dotted line). From Ref. 9.

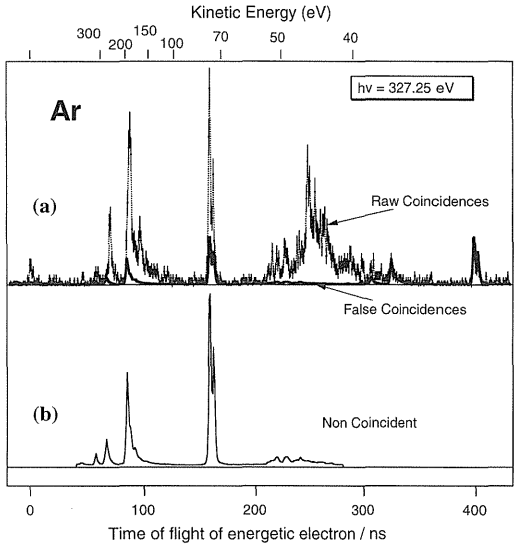

Figure 16. Argon. a) Raw and false threshold electron/energetic electron coincidence spectra obtained at $h\nu=327.25$ eV, corresponding to the maximum of emission of 2s threshold photoelectrons. b) Non coincident TOF spectrum of the energetic electrons at the same photon energy. Spectra have been obtained in a single bunch operation mode of Super ACO (240 ns between synchrotron light pulses).

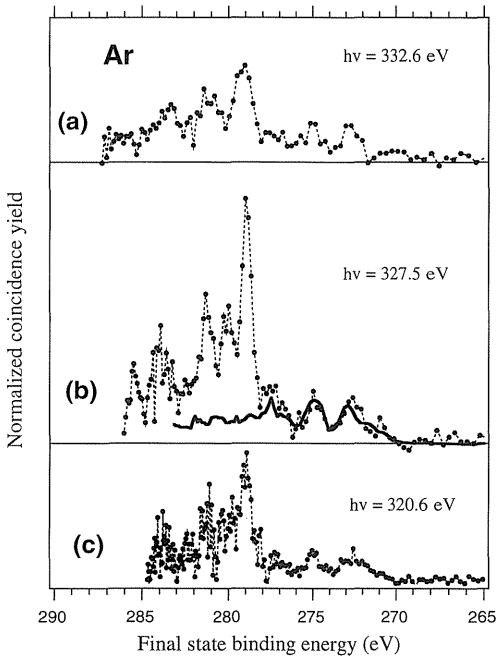

Figure 17. Coincident spectra taken for Ar, above (3a), below (3c), and on the Ar 2s threshold peak (3b). The three spectra are plotted on a common intensity scale. (Ref. 9).

As can be seen in **Fig. 12**, the 2s peak lies on a continuum, that corresponds to background 'noise' electrons and/or to real threshold electrons. The contribution of threshold Auger electrons associated with the 2p main line states and 2p satellites has just been discussed, but another contribution is present and is associated with a direct double photoionisation process, as is shown in **Fig. 17**: it compares coincident spectra taken above and below the Ar 2s threshold to that recorded on the 2s peak. The above mentioned structure associated with Auger threshold electrons and the 2p satellites keeps a fairly constant intensity in the three spectra. However, what is of particular interest is the coincidence signal at the Coster-Kronig line positions even when the 2s photoelectron is not selected. The fixed final state binding energy shows that it originates from the double photoionisation process:

$$h\nu+Ar\rightarrow Ar^{++}2p^{-1}3p^{-1}+e^-+e^-(E=0) \qquad (3)$$

where the Ar^{++} states are the same as those populated via the 2s hole by Coster-Kronig decay. The measurements in **Fig. 17** show an enhancement of reaction (3) by a factor of 3 ± 0.6 at the Ar 2s threshold, in other words, the 2s hole leads to an enhancement of the double photoionisation cross section to the $Ar^{++}2p^{-1}3p^{-1}$ states. From this result it is clear that, in these experiments, we are probing "resonance-affected" double ionisation, as defined by Krassig et al.[33]:

$$h\nu + Ar \rightarrow Ar^{++}2p^{-1}3p^{-1} + e^- + e^-(E=0) \quad (2)$$
$$\searrow \quad \swarrow$$
$$Ar^{+}2s^{-1} + e^-(E=0) \quad (4)$$

Note that the existence of the resonant process (4) has already been revealed in the experiment by Kylli et al[30], where they observe an increase of the cascade decay of the $Ar^{++}2p^{-1}3p^{-1}$ levels, when the Ar 2s channel is open.

These results on Ar 2s constitute a proof of principle for Auger/Threshold Photoelectron Coincidence Spectroscopy; they show the potential of this technique to study molecular dications, and their spectroscopy. Note that, because of the selection rules involved in a resonant process such as (4), electronic states different from those formed in a direct double ionisation process may be attained.

7. Conclusion

The spectacular progress made in the knowledge of dications has been illustrated by a few selected experimental examples. This progress was made possible by the conjunction of the development of synchrotron radiation sources on one hand and coincidence techniques on the other. Threshold electron spectrometers in particular, are very powerful experimental tools; their use together with a variety of coincidence techniques gives detailed information which was completely unknown only 10 years ago. It includes the vibrationally resolved spectroscopy of diatomic dications, the double photoionisation mechanisms and more. However, these techniques are just at their birth, and will certainly bring new insights on dications in the near future.

References

1) D. Mathur: Phys. Reports **225**, 193 (1993).
2) R. Dörner, H. Bräuning, J. M. Feagin, V. Mergel, O. Jagutzki, L. Spielberger, T. Vogt, H. Khemliche, M. H. Prior, J. Ullrich, C. L. Cocke and H. Schmidt-Böcking: Phys. Rev. **A 57**, 1074 (1998); V. Mergel, M. Achler, R. Dörner, Kh. Khayyat, T. Kambara, Y. Awaya, V. Zoran, B. Nyström, L. Spielberger, J. H. McGuire, J. Feagin, J. Berakdar, Y. Azuma and H. Schmidt-Böcking: Phys. Rev. Lett. **80**, 5301 (1998) *and references therein included.*
3) J. H. D. Eland: in *VUV phototionisation and photodissociation of molecules and clusters*; C. Y. Ng, Ed. World Scientific: (1991) p297; J. H. D. Eland and V. Schmidt: in *VUV and soft X-Ray Photoionization*, U. Becker and D. A. Shirley, Ed. Plenum Press, New York, (1996) p495.
4) P. Lablanquie, M. Lavollée, J. H. D. Eland, F. Penent and R. I. Hall: Meas. Sci. Technol. **7**, 939 (1995).
5) M. Hochlaf, H. Kjeldsen, F. Penent, R. I. Hall, P. Lablanquie, M. Lavollee and J. H. D. Eland: Can. J. Phys. **74**, 856 (1996).
6) S. Cvejanovic and F. H. Read: J. Phys. **B 7**, 1180 (1974).
7) F. Penent, R. I. Hall, R. Panajotovic, J. H. D. Eland, G. Chaplier and P. Lablanquie: Phys. Rev. Lett. **81**, 3619 (1998).
8) J. H. D. Eland: Meas. Sci. Technol. **4**, 1522 (1993).
9) P. Lablanquie, F. Penent, R. I. Hall, H. Kjeldsen, J. H. D. Eland, A. Muehleisen, P. Pelicon, Z. Smit, M. Zitnik and F. Koike: submitted (1999).
10) B. Langer, N. Berrah, R. Wehlitz, T. W. Gorczyca, J. Bozek and A. Farhat: J. Phys. **B 30**, 593 (1997); O. Hemmers, S. B. Whitfield, P. Glans, H. Wang, D. W. Lindle, R. Wehlitz and I. A. Sellin: Rev. Sci. Instrum. **69**, 3809 (1998).
11) R. I. Hall, A. McConkey, L. Avaldi, M. A. MacDonald and G. King: J. Phys. **B 25**, 411 (1992).
12) B. Krässig and V. Schmidt: J. Phys. **B 25**, L327 (1992).
13) G. C. King, L. Avaldi, G. Dawber, G. Stefani, M. Zitnik, M. A. Macdonald, and R. I. Hall: J. Elect. Spect. Rel. Phenom. **76**, 253 (1995) *and references therin included.*
14) B. Krässig, J. E. Hansen, W. Persson and V. Schmidt: J. Phys. **B 29**, L449 (1996).
15) U. Fano: J. Phys. **B 7**, L401 (1974).
16) M. Hochlaf, R. I. Hall, F. Penent, J. H. D. Eland and P. Lablanquie: Chem. Phys. **234**, 249 (1998).
17) D. Winkoun, G. Dujardin, L. Hellner and M. J. Besnard: J. Phys. **B 21**, 1385 (1988).
18) D. B. Thompson, G. Dawber, N. Guelly, M. A. MacDonald and G. C. King: J. Phys. **B 30**, L147 (1997).
19) J. H. D. Eland, P. Lablanquie, M. Lavollée, M. Simon, R. I. Hall, M. Hochlaf and F. Penent: J. Phys. **B 30**, 2177 (1997).
20) L. H. Andersen, J. H. Posthumus, O. Vahtras, H. Ågren, N. Elander, A. Nunez, Ascrinzi, M. Natiello and M. Larsson: Phys. Rev. Lett. **71**, 1812 (1993).
21) M. Lundqvist, P. Baltzer, D. Edvardsson, L. Karlsson and B. Wannerberg: Phys. Rev. Lett. **75**, 1058 (1995).
22) T. Baer et al.: in *VUV photoionisation and photodissociation of molecules and clusters*; C. Y. Ng, Ed. World Scientific: (1991) p259.
23) T. A. Field and J. H. D. Eland: Chem. Phys. Lett. **211**, 436 (1993).
24) T. A. Field: PhD Thesis, University of Oxford (1996).
25) P. Lablanquie, J. H. D. Eland, I. Nenner, P. Morin, J. Delwiche and M. J. Hubin-Franskin: Phys. Rev. Let. **58**, 992 (1987).
26) V. Schmidt: Rep. Prog. Phys. **55**, 1483 (1992); V. Schmidt: *Electron Spectroscopy of Atoms using Synchrotron Radiation* Cambridge University Press (1997).
27) S. D. Price and J. H. D. Eland: J. Phys. **B 24**, 4379 (1991).
28) T. J. Reddish, J. P. Wightman, M. A. MacDonald and S. Cvejanovic: Phys. Rev. Lett. **79**, 2438 (1997); R. Dörner, H. Bräuning, O. Jagutzki, V. Mergel, M. Achler, R. Moshammer, J. M. Feagin, T. Osipov, A. Bräuning-Demian, L. Spielberger, J. H. McGuire, M. H. Prior, N. Berrah, J. D. Bozek, C. L. Cocke and H. Schmidt-Böcking: Phys. Rev. Lett. **81**, 5776 (1998).
29) P. Bolognesi, D. B. Thompson, L. Avaldi, M. A. MacDonald, M. C. A. Lopes, D. R. Cooper and G. C. King: Phys. Rev. Lett. **82**, 2075 (1999).
30) T. Kylli, H. Aksela, O. P. Sairanen, A. Hiltunen and S. Aksela: J. Phys. **B 30**, 3647 (1997).
31) W. Mehlhorn: Z. Phys. **201**, 1 (1968).
32) P. Lablanquie, J. H. D. Eland, H. Kjeldsen, R. I. Hall, M. Hochlaf, R. Panajotovic, F. Penent and F. Combet-Farnoux: Abstracts, Int. Workshop on Photoionization (IWP'97) (Chester, UK, 1997) p96.
33) B. Krassig, O. Schwarzkopf and V. Schmidt: J. Phys. **B 26**, 2589 (1993).